C. R. Mecanique 341 (2013) 508–519

Contents lists available at SciVerse ScienceDirect

Comptes Rendus Mecanique

www.sciencedirect.com

Tension locking in finite-element analyses of textile composite reinforcement deformation

Verrouillage en tension lors de l'analyse par élément finis des déformations des renforts textiles de composites

Nahiène Hamila, Philippe Boisse *

Laboratoire de mécanique des contacts et des structures (LaMCoS), INSA de Lyon, bâtiment J. Jacquard, 69621 Villeurbanne cedex, France

ARTICLE INFO

Article history:
Received 6 May 2012
Accepted after revision 21 March 2013
Available online 11 April 2013

Keywords:
Composites
Textile reinforcement
Large shear strains
Finite element
Locking
Stabilisation

Mots-clés :
Composites
Renforts textiles
Grandes déformations de cisaillement
Éléments finis
Verrouillage
Stabilisation

ABSTRACT

The mechanical behaviour of textile composite reinforcements is characterised by a tensile stiffness in the two fibre directions, which is very large in comparison with the in-plane shear rigidity. The in-plane deformations of these materials are mainly due to the shear angle between warp and weft yarns. The finite-element analysis of these deformations leads to locking phenomena if the mesh is not aligned with the fibre directions. In this case the calculation gives spurious tensions in the fibres that make the analysis inaccurate. In the present paper, this phenomenon is highlighted and analysed in the case of the four-node finite element. In particular, a two-element example shows the impossibility of obtaining solutions without tensile strains for unaligned meshes. A solution to this tension locking is proposed for the four-node quadrilateral. It is based on a one-point quadrature and a specific stabilisation reduced to non-constant in-plane shear strains.

RÉSUMÉ

Le comportement mécanique des renforts de composites textiles est caractérisé par une rigidité en tension dans les deux directions de fibres très grande devant celle de cisaillement dans le plan. Les déformations dans le plan de ces matériaux sont principalement obtenues par changement d'angle entre les réseaux chaîne et trame. Lors d'une analyse par éléments finis de ces déformations, un phénomène de verrouillage apparaît lorsque le maillage n'est pas aligné avec les directions des fibres. Dans ce cas, le calcul conduit à des tensions erronées, qui perturbent l'analyse de façon majeure. Dans le présent article, ce phénomène est analysé dans le cas de l'élément fini à quatre nœuds. En particulier, un exemple à deux éléments montre l'impossibilité d'obtenir des solutions sans extensions des fibres pour des maillages quelconques. Une solution à ce problème de verrouillage est proposée pour le quadrangle à quatre nœuds. Elle utilise une intégration réduite et une stabilisation spécifique réduite aux termes de cisaillements plans non constants sur l'élément.

* Corresponding author.
E-mail addresses: nahiene.hamila@insa-lyon.fr (N. Hamila), philippe.boisse@insa-lyon.fr (P. Boisse).

1631-0721/$ – see front matter
http://dx.doi.org/10.1016/j.crme.2013.03.001

1. Introduction

Composites with continuous fibre textile reinforcements [1] bound with a thermoplastic or thermoset matrix are used to manufacture low-weight parts with strong stiffness and strength. The applications are numerous today in the field of aeronautics [2], automotive [3] or civil engineering [4]. The composite parts are generally thin, i.e. with a small thickness in comparison with the two other dimensions. Their shapes are often complex with double curvatures. To obtain these shapes, the initially plane fibrous reinforcement is formed on the surface. This forming is often called "draping" for textile reinforcement. In the case of double curve shapes, the draping process needs in-plane deformation of the reinforcement and especially in-plane shear strains. The reinforcement used for double curved parts are generally woven fabrics or NCF (Non-Crimp Fabrics). The warp and weft yarns permit large in-plane shear strains and the weaving (or the stitches in case of NCF) insures cohesion to the reinforcement during the shaping process. During the forming process, the matrix is absent or not hardened and in-plane shearing of the reinforcement is possible. The mechanical behaviour of textile reinforcement (dry textile or prepreg) is characterised by a very strong tensile stiffness in the two fibre directions. All the other rigidities are weak, especially the in-plane shear stiffness. The numerical simulations of textile reinforcement forming processes are important in order to determine the conditions for a successful draping and to know the direction of the fibres in the part. To simulate draping of textile composite reinforcement, several software packages have been developed based on "kinematical models" [5,6]. This method is very fast, but does not take into account two important points: the mechanical behaviour of the woven reinforcement and the load boundary conditions. Consequently, some draping simulations have been developed in the framework of the finite-element method [7–9]. The reinforcement is considered as a continuous material with a specific mechanical behaviour [10–13].

An important problem in FE simulation of fibre reinforcement has been identified by Yu et al. [14,15]. The in-plane shear deformation of textile reinforcement can lead to spurious tensions (or compressions) in the fibres for arbitrary meshes. The specificity of the textile reinforcement that leads to this phenomenon is the very large tensile stiffness of the fibres in comparison with the in-plane shear stiffness that is close to zero. These spurious tensions vanish if the mesh is aligned with the yarn directions. This problem is important because the use of meshes aligned with the element can be not convenient, in particular when the fibres are not aligned with the edges of the ply. It also renders impossible the use of automatic meshing and remeshing. In practice it is impossible to use a mesh that leads to spurious tensions for a draping simulation because these tensions lead to spurious wrinkles.

The development of these spurious tensions falls within the finite-element locking phenomena. This locking appears because the finite-element interpolation and the physics of the textile reinforcement are not compatible. This incompatibility leads to a far too stiff behaviour. There are several other locking phenomena. Volumetric locking of 2D and 3D finite elements [16–19], shear locking of quadrilaterals in-plane bending [17–19], transverse shear of plate elements [20–22], membrane locking of shell elements [23–25] have been intensively studied in the last decades to propose solutions to avoid these locking phenomena.

The locking in FE simulations of textile reinforcement deformation has been called "intra-ply shear locking" in [14,15]. Nevertheless, the reasons for this locking are spurious tensions in the yarns. In order to be consistent with the other locking phenomena, this locking will be called "tension locking" in the present paper. All the locking phenomena listed above have the name of the spurious energy leading to locking.

In the present paper, the tension locking during simulations of textile reinforcement in-plane deformation is highlighted. The analysis is carried out for different four-node quadrilateral meshes. The deformation of an initially rectangular textile reinforcement strip on a circular part is taken as an example. It leads to an in-plane shear that is variable in the deformed reinforcement. The tension locking is highlighted in the case of unaligned meshes. The reasons for the locking are analysed on a two-element mesh. Then a solution to avoid tension locking is proposed. It is based on a one-point quadrature and a specific stabilisation of the hourglass modes. The hourglass control concerns the in-plane shear angle between warp and weft fibres and is orthogonal to any tensile strains. It is shown that this approach avoids the tensile locking phenomena highlighted with the full integration. In addition, the proposed procedure is numerically efficient, because it is based on a one-point quadrature. Some multi-field elements have been proposed in [26] in order to avoid locking of textile reinforcements. These elements involve both displacements and strain degrees of freedom. This is very numerically costly and cannot be used in dynamic explicit approaches.

2. Highlighting and analysis of tension locking

2.1. Mechanical behaviour of textile composite reinforcements

The specificities of the fibre reinforcement's mechanical behaviour come from their internal structure. Textiles are composed of warp and weft tows, themselves made up of thousands of fibres (Fig. 1). A key consequence of this structure is the possible relative motions between fibres and between yarns that leads to a very specific mechanical behaviour. The only high stiffness is the tensile stiffness in the fibre direction. All the other rigidities (in-plane shear, bending, and compaction) are much weaker. Depending on the specific application of interest, the analyses of these textile reinforcements can be made at the microscopic scale, i.e. the scale of the fibre (Fig. 1c) or at the mesoscopic scale, i.e. the scale of the unit woven cell (Fig. 1b) or at the macroscopic scale, i.e. the scale of the part (Fig. 1a). If some local analyses are made at the microscopic

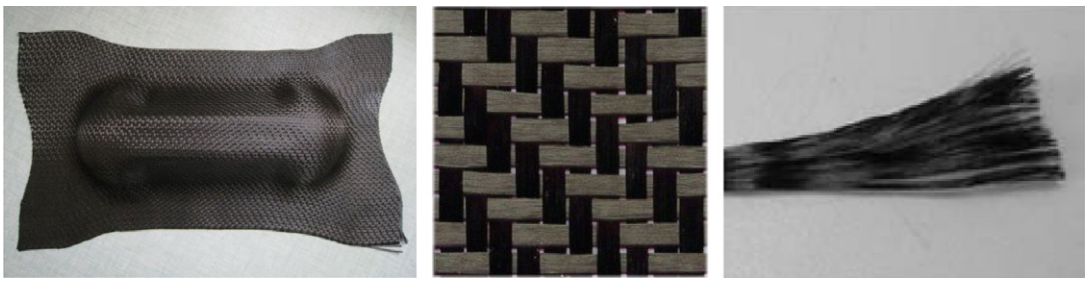

Fig. 1. The different scales of the textile composite reinforcements.

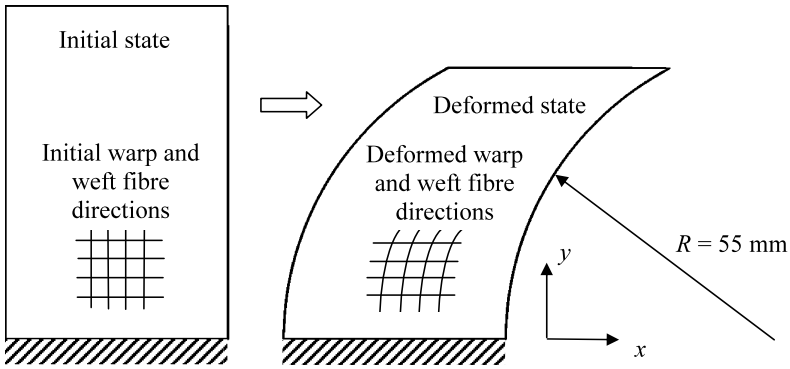

Fig. 2. Deformation of a textile reinforcement strip on a circular obstacle.

[27] or the mesoscopic scale [28], the forming simulations of the textile preforms are performed at the macroscopic scale in most cases [7–9]. The textile reinforcement is meshed by finite elements made of fibrous materials. The rigidities in the directions of the warp yarns and weft yarns are very large in comparison to all the other stiffnesses.

2.2. Tension locking in a textile strip deformation

The in-plane deformation of a 40 mm $\times$ 60 mm rectangular woven textile strip is analysed (Fig. 2). The inferior edge of the strip is clamped. The displacement in the x direction (horizontal) is prescribed on the right edge to reach a 55-mm circle without stretching of the vertical fibre on the right edge. The warp and weft yarns are in the x and y directions in the initial state (horizontal and vertical). The yarns are assumed to be elastic. Their stiffness in the warp and weft direction is 10^4 N/mm. The in-plane shear stiffness is assumed to be equal to zero. Consequently, the deformation of the fabric strip is performed without force and the tensions and tensile strains in the fibres must be equal to zero. The calculations are performed with standard 4-node quadrilaterals implemented in the code Plasfib [9]. The in-plane shear angle is zero at the bottom of the strip and reaches 60° at the top of the deformed strip. It is continually variable in the height of the strip. The fabric strip is meshed with four node elements. First, a rectangular mesh aligned with the warp and weft fibres is used (Fig. 3). The computed stretching strains in the warp and weft fibres are equal to zero (inferior to 2×10^{-6}).

In a second time, the strip is meshed with irregular elements (Fig. 4). Consequently, the edges of the elements are no more aligned with the warp and weft directions. The computed stretching strains in the warp and weft yarns are much larger (up to 9.5×10^{-3}). These tensile strains in the yarns lead to spurious tensions and loads on the right edge are necessary to perform the deformation. Fig. 5 shows the resultant load on the strip during the deformation in function of the horizontal displacement at the top of the strip.

This load is almost zero with the aligned mesh, but it reaches 140 N with the irregular mesh. These tensions in the yarns and loads required to shape the strip are spurious loads since the in-plane shear stiffness of the textile reinforcement is equal to zero. They are due to the inability of the 4-node quadrilateral to obtain solutions without tensile strains in the fibre directions when the mesh is unaligned. This inability of finite elements made up of textile material to compute the in-plane deformation when the elements are not aligned with the warp and weft fibre directions is the tension locking phenomenon. This phenomenon has been highlighted in some other situations, in particular in the case of the bias extension test and cylindrical cup forming [14,15].

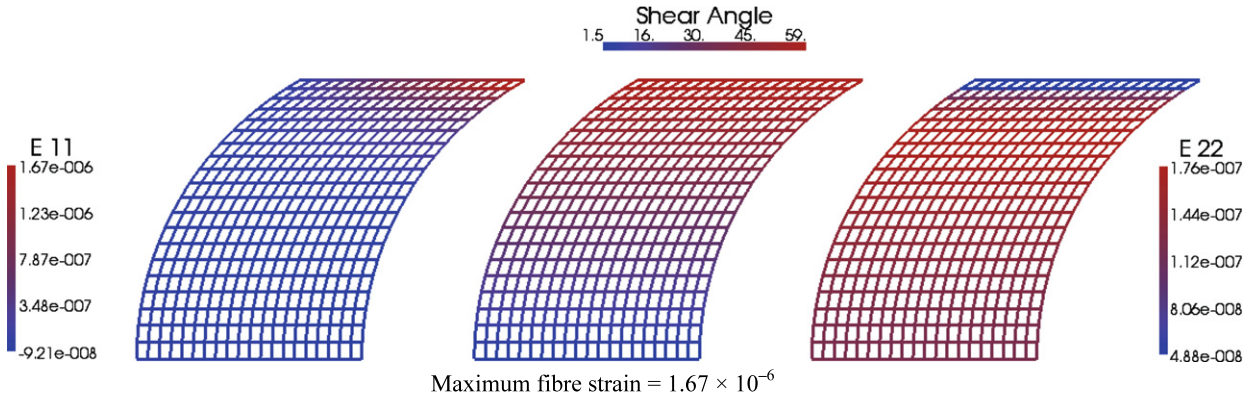

Fig. 3. Simulation of the deformation of a textile reinforcement strip using an aligned mesh. Tensile strain in the warp and weft yarns and shear angles.

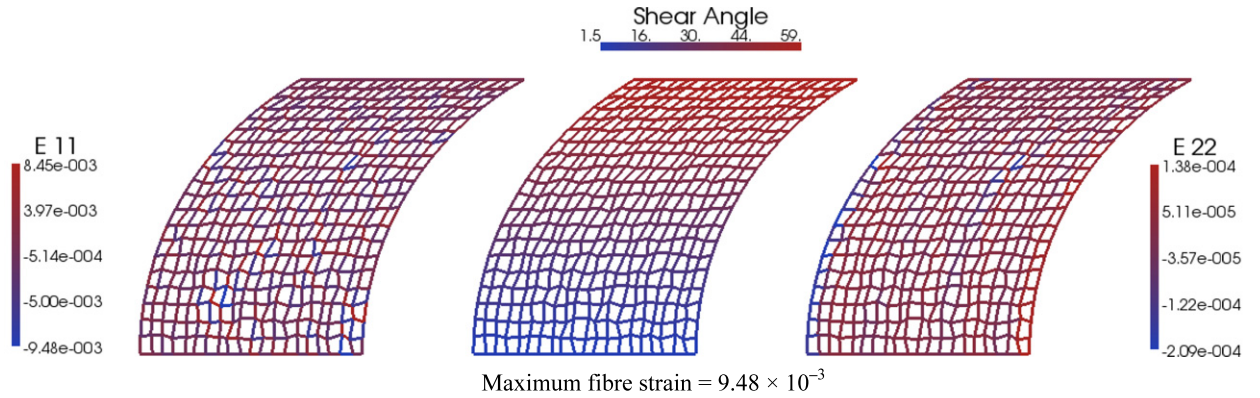

Fig. 4. Simulation of the deformation of a textile reinforcement strip using an irregular mesh. Tensile strain in the warp and weft yarns and shear angles.

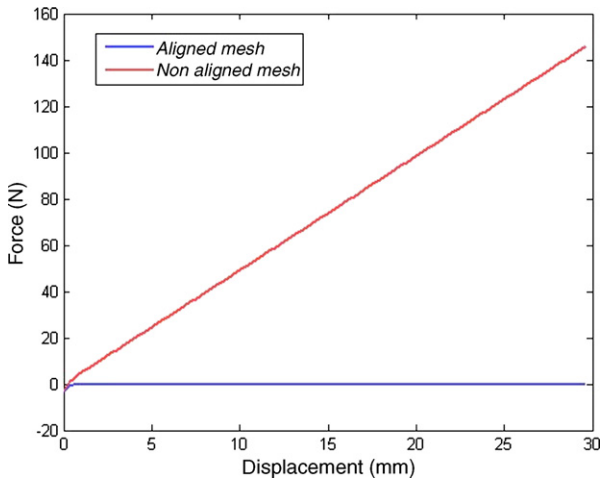

Fig. 5. Load on the textile reinforcement strip during the deformation. Aligned mesh: blue; non-aligned mesh: red.

2.3. Tension locking in a two-element mesh

A set of two elements is considered in order to analyse the reasons for the tension locking. A textile reinforcement strip is meshed with two elements (Fig. 6). The nodes 1 and 2 are clamped. The fibres are oriented in the $\mathbf{e}_1$ and $\mathbf{e}_2$ directions (horizontal and vertical). The side 1–2 must be in a fibre direction, otherwise the reinforcement is blocked in its entirety. The question is whether it is possible to prescribe nodes 3 and 6 velocities that lead to a deformed state of the same nature as those of Fig. 3. In other words, is it possible to prescribe independent velocities in 3 and 6 without tension in the fibres? The directions of the fibres are denoted $\mathbf{k}_1$ and $\mathbf{k}_2$. In the initial position, $\mathbf{k}_1 = \mathbf{e}_1$ and $\mathbf{k}_2 = \mathbf{e}_2$. At a point M, the material

	x	y
Node 1	0	0
Node 2	2	0
Node 3	2	3
Node 4	0	2
Node 5	0	5
Node 6	2	5

Coordinates of the nodes

Element A (inferior): (1,2,3,4)

Element B (superior): (4,3,6,5)

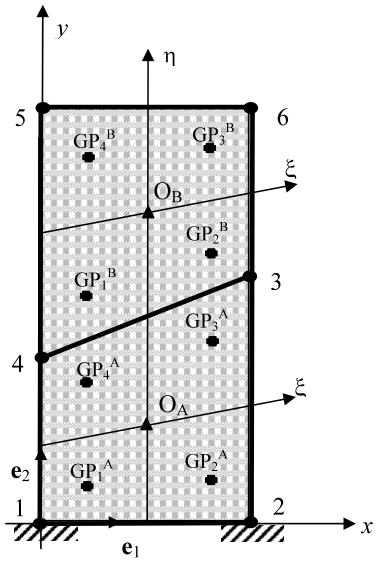

Fig. 6. Set of two 4-node elements made up of textile reinforcement.

coordinates $\xi \in [-1, 1]$ and $\eta \in [-1, 1]$ are used to define the interpolation of the displacement (or velocity) and position. The interpolation function of the node i ($i \in [1, 4]$) is:

$$N_i(\xi, \eta) = 1/4(1 - \xi_i\xi)(1 - \eta_i\eta) \tag{1}$$

The material covariant vectors are obtained from the derivation of the position $\mathbf{x}$ of a point M with respect to ξ and η.

$$\mathbf{g}_1 = \frac{\partial \mathbf{x}}{\partial \xi} = \frac{\partial N_i}{\partial \xi}\mathbf{x}_i, \qquad \mathbf{g}_2 = \frac{\partial \mathbf{x}}{\partial \eta} = \frac{\partial N_i}{\partial \eta}\mathbf{x}_i \tag{2}$$

The related contravariant vectors $\mathbf{g}^\alpha$ are such as:

$$\mathbf{g}^\alpha \cdot \mathbf{g}_\beta = \delta^\alpha_\beta$$

α and β take the value 1 or 2.

The inextensibility conditions in the directions $\mathbf{k}_1$ and $\mathbf{k}_2$ are:

$$\mathbf{k}_1 \cdot \dot{\mathbf{k}}_1 = 0, \qquad \mathbf{k}_2 \cdot \dot{\mathbf{k}}_2 = 0$$

where $\dot{X}$ is the time derivative of a quantity X.

Taking into account the fibre orientations in the stripe (Fig. 6),

$$g^1_x \dot{g}_{1x} + g^2_x \dot{g}_{2x} = 0, \qquad g^1_y \dot{g}_{1y} + g^2_y \dot{g}_{2y} = 0$$

where $a_x = \mathbf{a} \cdot \mathbf{e}_1$ and $a_y = \mathbf{a} \cdot \mathbf{e}_2$. These inextensibility conditions are written at the Gauss points of the elements such as $\xi = \pm\frac{1}{\sqrt{3}}$, $\eta = \pm\frac{1}{\sqrt{3}}$ (GP_1 to GP_4 in Fig. 6).

2.3.1. Element A

Taking into account Eqs. (1) and (2), the material covariant vectors $\mathbf{g}_1$ and $\mathbf{g}_2$ in the element A have the following form:

$$\mathbf{g}_1 = \frac{1}{4}\big[(1 - \eta)(\mathbf{x}_2 - \mathbf{x}_1) + (1 + \eta)(\mathbf{x}_3 - \mathbf{x}_4)\big]$$

$$\mathbf{g}_2 = \frac{1}{4}\big[(1 - \xi)(\mathbf{x}_4 - \mathbf{x}_1) + (1 + \xi)(\mathbf{x}_3 - \mathbf{x}_2)\big]$$

Taking the clamping of nodes 1 and 2 into account, the inextensibility conditions in the element A are:

$$\big[g^1_x(1 + \eta) + g^2_x(1 + \xi)\big]u_3 + \big[-g^1_x(1 + \eta) + g^2_x(1 - \xi)\big]u_4 = 0 \tag{3.1}$$

$$\big[g^1_y(1 + \eta) + g^2_y(1 + \xi)\big]v_3 + \big[-g^1_y(1 + \eta) + g^2_y(1 - \xi)\big]v_4 = 0 \tag{3.2}$$

where the velocity of a node i is $\mathbf{v}_i = u_i\mathbf{e}_1 + v_i\mathbf{e}_2$. These equations written at the four Gauss points give two systems of four scalar equations with two unknowns each. The first one concerns the horizontal velocity components u_3 and u_4 and the second one concerns the horizontal velocity components v_3 and v_4.

$$0.38225928u_3 - 0.57338893u_4 = 0 \tag{4.1}$$

$$0.30311866u_3 - 0.45467799u_4 = 0 \tag{4.2}$$

$$1.13125423u_3 - 1.69688134u_4 = 0 \tag{4.3}$$

$$1.42661107u_3 - 2.13991661u_4 = 0 \tag{4.4}$$

$$0.38225928v_3 + 1.42661107v_4 = 0 \tag{5.1}$$

$$1.13125423v_3 + 0.30311866v_4 = 0 \tag{5.2}$$

$$1.13125423v_3 + 0.30311866v_4 = 0 \tag{5.3}$$

$$0.38225928v_3 + 1.42661107v_4 = 0 \tag{5.4}$$

The equations of the first system ((4.1) to (4.4)) concerning the horizontal velocity components u_3 and u_4 are dependent. These four equations are equivalent to $u_3 = 1.5u_4$.

The equations of the second system ((5.1) to (5.4)) concerning the vertical velocity components v_3 and v_4 are not all dependent; consequently $v_3 = v_4 = 0$.

It is therefore possible to prescribe a horizontal velocity, for instance at node 3, and all the velocities of the element A are fixed and verify the fibre inextensibility.

2.3.2. Element B

Taking into account (1) and (2), the vectors $\mathbf{g}_1$ and $\mathbf{g}_2$ in element B have the following form:

$$\mathbf{g}_1 = \frac{1}{4}\big[(1-\eta)(\mathbf{x}_3 - \mathbf{x}_4) + (1+\eta)(\mathbf{x}_5 - \mathbf{x}_6)\big]$$

$$\mathbf{g}_2 = \frac{1}{4}\big[(1-\xi)(\mathbf{x}_5 - \mathbf{x}_4) + (1+\xi)(\mathbf{x}_6 - \mathbf{x}_3)\big]$$

The inextensibility conditions in element B are:

$$\begin{aligned}&\big[-g_x^1(1+\eta) + g_x^2(1-\xi)\big]u_5 + \big[g_x^1(1+\eta) + g_x^2(1+\xi)\big]u_6 \\ &\quad = \big[-g_x^1(1-\eta) + g_x^2(1+\xi)\big]u_3 + \big[g_x^1(1-\eta) + g_x^2(1-\xi)\big]u_4\end{aligned} \tag{6.1}$$

$$\begin{aligned}&\big[-g_y^1(1+\eta) + g_y^2(1-\xi)\big]v_5 + \big[g_y^1(1+\eta) + g_y^2(1+\xi)\big]v_6 \\ &\quad = \big[-g_y^1(1-\eta) + g_y^2(1+\xi)\big]v_3 + \big[g_y^1(1-\eta) + g_y^2(1-\xi)\big]v_4\end{aligned} \tag{6.2}$$

Taking into account that $u_4 = \frac{u_3}{1.5}$ and denoting $w_5 = \frac{u_5}{u_3}$ and $w_6 = \frac{u_6}{u_3}$, Eq. (6.1) gives, at the four Gauss points:

$$-0.86874577w_5 + 0.30311866w_6 = -0.94271186 \tag{7.1}$$

$$-0.57338893w_5 - 0.13991661w_6 = -1.18884256 \tag{7.2}$$

$$-1.61774072w_5 + 1.42661107w_6 = -0.3185494 \tag{7.3}$$

$$-1.69688134w_5 + 1.54532201w_6 = -0.25259888 \tag{7.4}$$

The rank of the four Eqs. (7.1) to (7.4) is 2. They lead to:

$$w_5 = w_6 = 1.66667, \quad \text{i.e.} \quad u_5 = u_6 = 1.66667u_3$$

Taking $v_3 = v_4 = 0$ into account, the four-equation system given by (6.2) is a homogeneous system with a determinant different from zero, consequently $v_5 = v_6 = 0$.

This highlights the tension locking of this two-element set. In the same way, it is not possible to obtain a deformation such as those of Figs. 3 and 4 without tensions of the fibres. Only the deformation of Fig. 7a is possible when the inextensibility conditions are verified (constant shear angle within the two elements). Any deformation of the type of those shown in Fig. 7b is impossible without fibre tensile strain.

2.3.3. Aligned two-element mesh

The same analysis is made in the case of a two-element mesh aligned with the fibre directions (Fig. 8a). In this case, the system (4.1) to (4.4) leads to $u_3 = u_4$, the system (5.1) to (5.4) still imposes $v_3 = v_4 = 0$. In the system (7.1) to (7.4) corresponding to the inextensibility in the $\mathbf{k}_1$ direction, the second member is equal to zero and the four equations give $u_5 = u_6$. Consequently, it is possible to have a deformation of element B independent from those of element A and with a different angle between the fibres (Fig. 7c). This situation is similar to those of Fig. 3 using an aligned mesh for the reinforcement strip that can be deformed without tensions.

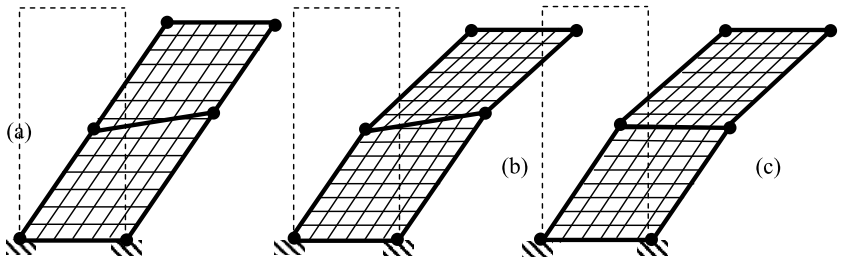

Fig. 7. Deformation of a two-element mesh. (a) Deformation without fibre tensions. (b) Deformation impossible without fibre tensions. (c) Deformation possible without tensions in the case of aligned elements.

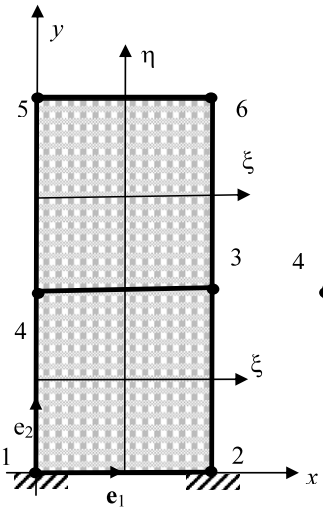

(a)

	x	y
Node 1	0	0
Node 2	2	0
Node 3	2	2.5
Node 4	0	2.5
Node 5	0	5
Node 6	2	5

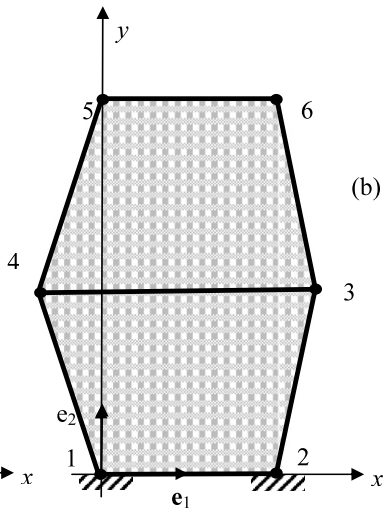

(b)

	x	y
Node 1	0	0
Node 2	2	0
Node 3	2.5	2.5
Node 4	−1	2.5
Node 5	0	5
Node 6	2	5

Fig. 8. (a) Aligned two-element mesh. (b) Horizontally aligned two-element mesh.

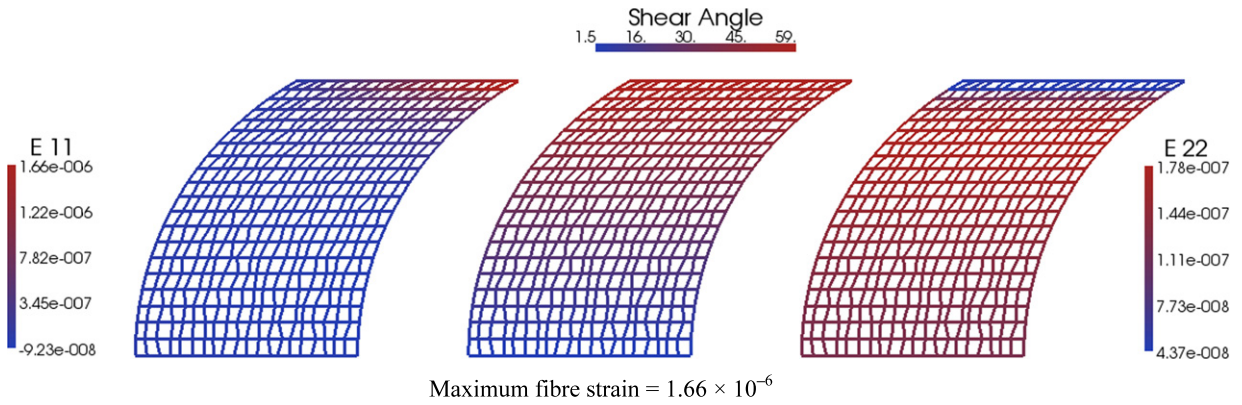

Fig. 9. Absence of tension locking in the case of a horizontally aligned mesh.

2.3.4. Horizontally aligned two-element mesh

The alignment of elements with the fibres is only necessary in the horizontal direction (those of the clamping of nodes 1 and 2). The two-element mesh defined in Fig. 8b leads to a system (7.1) to (7.4) with a second member equal to zero and permits an independent horizontal velocity $u_5 = u_6$. This is confirmed in Fig. 9 by a simulation of the deformation of the textile reinforcement strip meshed with elements only aligned in the horizontal direction. There is no tension locking in this case. If the mesh is aligned only in the vertical direction, tension locking occurs (Fig. 10).

2.3.5. One-point quadrature elements

The 2×2 quadrature elements used above lead to inextensibility conditions that cannot be simultaneously verified in most deformation field in the case of an arbitrary geometry of the element relatively to the fibre directions. This is the

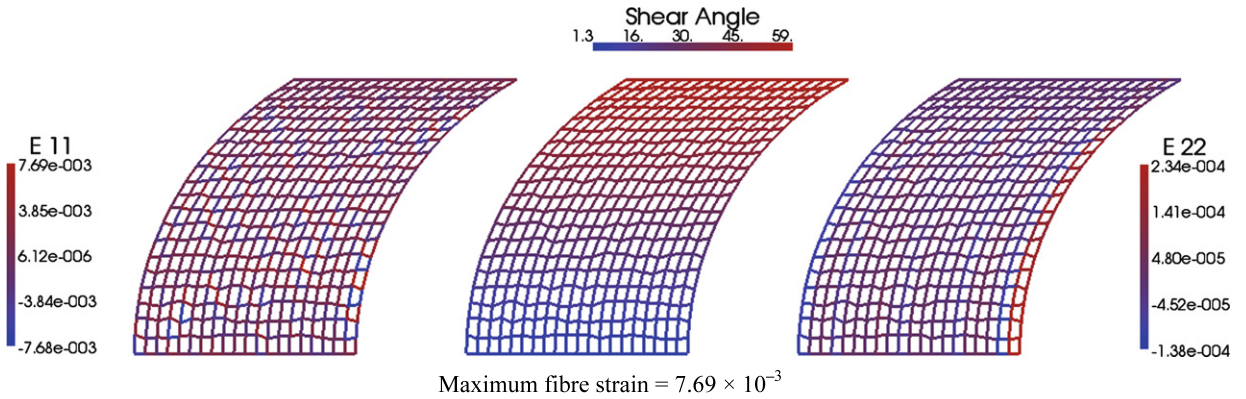

Fig. 10. Tension locking in the case of a vertically aligned mesh.

reason for tension locking in the case of textile reinforcement materials. For several locking phenomena, the underintegration has proved to be a possible solution to avoid locking, because the number of constraints is reduced in this approach. It is analysed in the case of the textile reinforcement deformation. The two elements defined in Fig. 6 are considered with one-point quadrature.

In element A, the inextensibility conditions (3.1) and (3.2) are written at the centre O_A of the element ($\xi = \eta = 0$). The inextensibility in the $\mathbf{k}_1$ direction (3.1), gives:

$$0.8u_3 - 1.2u_4 = 0$$

This equation is the same as Eqs. (4.1) to (4.4), given by the horizontal inextensibility in case of 2×2 quadrature.

The inextensibility in the $\mathbf{k}_2$ direction leads to:

$$v_3 = -v_4 \tag{8}$$

There is only one equation for two unknowns in both directions (rank = 1 for the two systems with two unknowns). The inextensibility of the fabric on the whole element leads to $v_3 = v_4 = 0$. This is possible in Eq. (8), but this is not ensured by the one-point quadrature, and spurious modes (hourglass) can develop.

In element B, the inextensibility condition in the $\mathbf{k}_1$ direction at point O_B gives:

$$-1.2w_5 + 0.8w_6 = -2/3$$

Consequently, it is possible to prescribe an arbitrary velocity u_6 while verifying the inextensibility condition. This FE solution may not be the exact solution (in the present case, the exact solution requires $w_5 = w_6$), but it does not lead to spurious tensions in a situation such as that in Fig. 7b.

The inextensibility condition in the $\mathbf{k}_2$ direction (6.2) at point O gives:

$$0.8z_5 + 0.8z_6 = 1.6$$

where $z_5 = \frac{v_5}{v_3}$ and $z_6 = \frac{v_6}{v_3}$.

Similarly to element A (rank = 1 for the two systems with two unknowns), there are possible spurious vertical velocities of nodes 5 and 6 that do not lead to tensile strains at point O.

In conclusion, the one-point quadrature is a possibility to avoid tension locking of quadrilateral made of stiff fibres. Nevertheless, in this case, the 4-node element is rank-deficient [19,29]. A stabilisation procedure is proposed in the next section for the one-point quadrature 4-node element made up of textile reinforcement in order to avoid tension locking without spurious modes.

3. Hourglass control

3.1. Interpolation of the velocity gradient

It has been shown in Section 2.3.5 that reduced integration can avoid tension locking of the 4-node finite element. Unfortunately, spurious zero energy mode can develop and the direct use of the one-point quadrature element is not possible. Stabilisation procedures have been proposed [19,29] and are used in F. E. codes for standard materials but these methods do not work well for very anisotropic materials and especially in the case of textile composite reinforcements that are considered in the present study. A stabilisation procedure is proposed for the 4-node quadrilateral element made of fibres in two directions using a one-point quadrature. It only concerns the in-plane shear strain energy.

The gradient matrices at the centre of the element ($\xi = \eta = 0$) are defined as:

$$\mathbf{b}_x^{\mathrm{T}} = \mathbf{N},_x = \frac{1}{2A}[y_2 - y_4, y_3 - y_1, y_4 - y_2, y_1 - y_3]$$
$$\mathbf{b}_y^{\mathrm{T}} = \mathbf{N},_y = \frac{1}{2A}[x_4 - x_2, x_1 - x_3, x_2 - x_4, x_3 - x_1]$$

A is the area of the element. For the purpose of hourglass control, the $\boldsymbol{\gamma}$ vector is introduced [17–19]:

$$\boldsymbol{\gamma} = \frac{1}{4}\big(\mathbf{h} - (\mathbf{h}^{\mathrm{T}}\mathbf{x})\mathbf{b}_x - (\mathbf{h}^{\mathrm{T}}\mathbf{y})\mathbf{b}_y\big), \qquad \bar{\mathbf{1}} = \frac{1}{4}\big(\mathbf{1} - (\mathbf{1}^{\mathrm{T}}\mathbf{x})\mathbf{b}_x - (\mathbf{1}^{\mathrm{T}}\mathbf{y})\mathbf{b}_y\big)$$

where $\mathbf{1}^{\mathrm{T}} = [1, 1, 1, 1]$ and $\mathbf{h}^{\mathrm{T}} = [1, -1, 1, -1]$. $\mathbf{h}$ is the matrix of the nodal values of $h = \xi\eta$.

A main interest of the $\boldsymbol{\gamma}$ vector is that it is orthogonal to all linear fields [19].

Let us consider the velocity of a point M, $\mathbf{v}(\mathrm{M}) = u\mathbf{e}_1 + v\mathbf{e}_2$. Within the 4-node quadrilateral element with bilinear interpolation, the velocity components can be written under the form:

$$u = \alpha_{x0} + \alpha_{x1}x + \alpha_{x2}y + \alpha_{x3}h$$
$$v = \alpha_{y0} + \alpha_{y1}x + \alpha_{y2}y + \alpha_{y3}h$$

Denoting $\mathbf{u}$ and $\mathbf{v}$ the column matrices of the nodal velocity components, the orthogonality properties lead to [19]:

$$u = (\bar{\mathbf{1}}^{\mathrm{T}}\mathbf{u}) + (\mathbf{b}_x^{\mathrm{T}}\mathbf{u})x + (\mathbf{b}_y^{\mathrm{T}}\mathbf{u})y + (\boldsymbol{\gamma}^{\mathrm{T}}\mathbf{u})h$$
$$v = (\bar{\mathbf{1}}^{\mathrm{T}}\mathbf{v}) + (\mathbf{b}_x^{\mathrm{T}}\mathbf{v})x + (\mathbf{b}_y^{\mathrm{T}}\mathbf{v})y + (\boldsymbol{\gamma}^{\mathrm{T}}\mathbf{v})h$$

The components of the velocity gradient $\mathbf{L}$ in the frame $(\mathbf{e}_1, \mathbf{e}_2)$ can be interpolated as a function of the nodal velocities:

$$\begin{bmatrix} L_{xx} = u,_x \\ L_{yy} = v,_y \\ L_{xy} = u,_y \\ L_{yx} = v,_x \end{bmatrix} = (\mathbf{B}_{0\mathrm{L}} + \mathbf{B}_{\mathrm{HGL}}) \begin{bmatrix} \mathbf{u} \\ \mathbf{v} \end{bmatrix}$$

with

$$\mathbf{B}_{0\mathrm{L}} = \begin{bmatrix} \mathbf{b}_x^{\mathrm{T}} & 0 \\ 0 & \mathbf{b}_y^{\mathrm{T}} \\ \mathbf{b}_y^{\mathrm{T}} & 0 \\ 0 & \mathbf{b}_x^{\mathrm{T}} \end{bmatrix}, \qquad \mathbf{B}_{\mathrm{HGL}} = \begin{bmatrix} h,_x\boldsymbol{\gamma}^{\mathrm{T}} & 0 \\ 0 & h,_y\boldsymbol{\gamma}^{\mathrm{T}} \\ h,_y\boldsymbol{\gamma}^{\mathrm{T}} & 0 \\ 0 & h,_x\boldsymbol{\gamma}^{\mathrm{T}} \end{bmatrix}$$

3.2. Stabilisation procedure

The stabilisation is made on the in-plane shear deformation mode. The angle variation between the warp and weft fibres due to the deformation is denoted Γ [30]. This in-plane shear angle is the principal kinematical quantity that permits to form the textile reinforcement on double curve shapes [1,30].

$\mathbf{f}_1$ and $\mathbf{f}_2$ are the vectors with a norm equal to 1 in the warp and weft fibre directions. $\mathbf{f}^1$ and $\mathbf{f}^2$ vectors such as $\mathbf{f}_1 \cdot \mathbf{f}^2 = \mathbf{f}_2 \cdot \mathbf{f}^1 = 0$ with a norm equal to 1. The shear angle velocity $\dot{\Gamma}$ is related to the velocity gradient [31]:

$$\dot{\Gamma} = \mathbf{f}^2 \cdot \mathbf{L} \cdot \mathbf{f}_1 + \mathbf{f}^1 \cdot \mathbf{L} \cdot \mathbf{f}_2 = \mathbf{f}^{\mathrm{T}}(\mathbf{B}_{0\mathrm{L}} + \mathbf{B}_{\mathrm{HGL}}) \begin{bmatrix} \mathbf{u} \\ \mathbf{v} \end{bmatrix}$$

where

$$\mathbf{f}^{\mathrm{T}} = \begin{bmatrix} f_x^2 f_{1x} + f_x^1 f_{2x} & f_y^2 f_{1y} + f_y^1 f_{2y} & f_x^2 f_{1y} + f_x^1 f_{2y} & f_y^2 f_{1x} + f_y^1 f_{2x} \end{bmatrix}$$

The in-plane shear internal virtual power on the element is:

$$P_{\mathrm{int}}^{*\mathrm{se}} = \mathbf{v}^{*\mathrm{T}}\mathbf{F}_{\mathrm{int}}^{\mathrm{se}} = \int_{S^e} \dot{\Gamma}^* M_s \, \mathrm{d}S$$

M_s is the moment per surface unit due to in-plane shear. $\mathbf{F}_{\mathrm{int}}^{\mathrm{se}}$ is the in-plane shear nodal load vector. Consequently,

$$\mathbf{F}_{\mathrm{int}}^{\mathrm{se}} = \int_{S^e} (\mathbf{B}_{0\mathrm{L}}^{\mathrm{T}} + \mathbf{B}_{\mathrm{HGL}}^{\mathrm{T}})\mathbf{f} M_s \, \mathrm{d}S$$

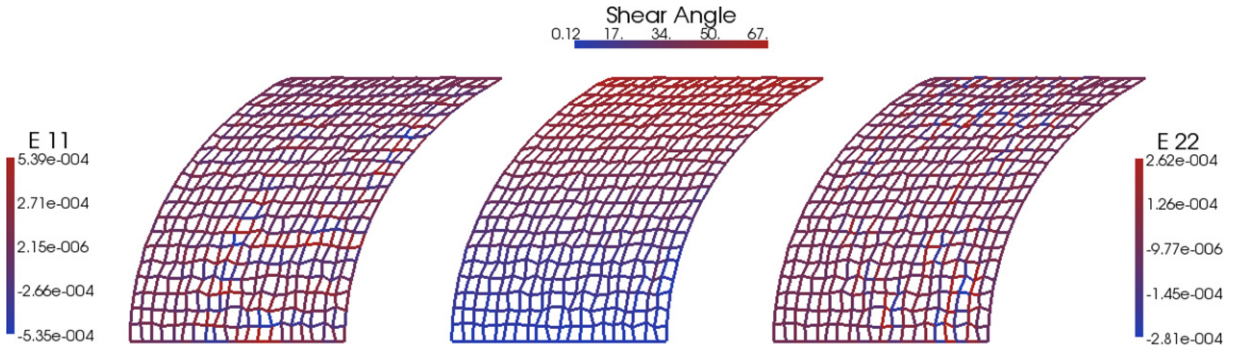

(a) $C_s = 1$; maximum fibre strain = 5.39×10^{-4}

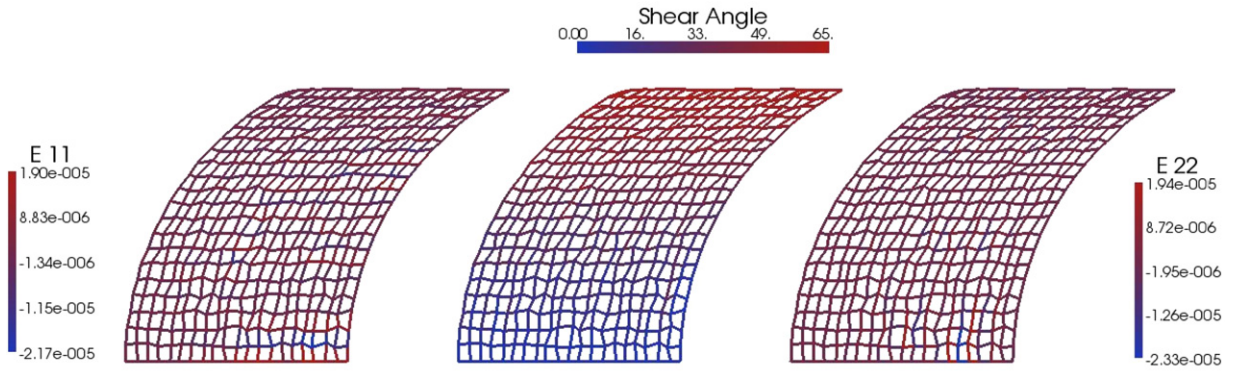

(b) $C_s = 0.01$; maximum fibre strain = 2.33×10^{-5}

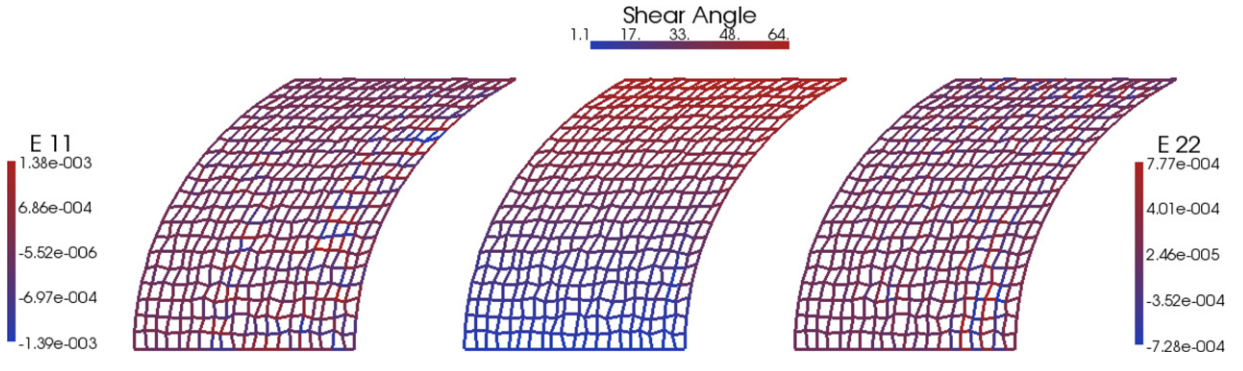

(c) $C_s = 10$; Maximum fibre strain = 1.39×10^{-3}

Fig. 11. Simulation of the deformation of a textile reinforcement strip using an irregular mesh and one-point quadrature and stabilisation for three different parameters C_s.

A one-point quadrature is used for the first term:

$$\mathbf{F}_{\text{int}}^{\text{se}} = A\mathbf{B}_{0\text{L}}^{\text{T}}(0)\mathbf{f}(0)M_s(0) + \mathbf{F}_{\text{stab}}^{\text{se}}$$

The second term defines the stabilisation nodal force matrix $\mathbf{F}_{\text{stab}}^{\text{se}}$:

$$\mathbf{F}_{\text{stab}}^{\text{se}} = \int_{S^e} \mathbf{B}_{\text{HGL}}^{\text{T}}\mathbf{f}\widetilde{M}_s \,\mathrm{d}S = \frac{A}{4}\sum_{k=1}^{4} \mathbf{B}_{\text{HGL}k}^{\text{T}}\mathbf{f}_k\widetilde{M}_{sk}$$

at time t_i, denoting $\Delta t = t_i - t_{i-1}$

$$\widetilde{M}_s(t_i) = \widetilde{M}_s(t_{i-1}) + \dot{\widetilde{M}}_s\Delta t$$

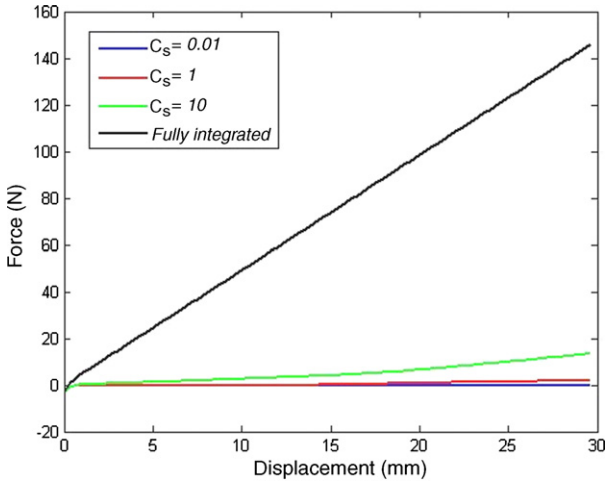

Fig. 12. Load on the textile reinforcement strip during the deformation with different approaches. Top to bottom: fully integrated, $C_s = 10$, $C_s = 1$, $C_s = 0.01$.

with

$$\tilde{\dot{M}}_s = C_s \mathbf{f}^T \mathbf{B}_{HGL}^T \begin{bmatrix} \mathbf{u} \\ \mathbf{v} \end{bmatrix}$$

The stabilisation nodal force matrix only concerns the non-constant part of the in-plane shear. The objective of the parameter C_s is to stabilise the quadrilateral but not to overwhelm the one-point quadrature stiffness.

3.3. Textile strip deformation

The stabilisation procedure defined in Section 3.2 is used to analyse the textile strip deformation defined in Section 2.3. Three values of the parameter C_s are considered: $C_s = 1$, $C_s = 0.01$ and $C_s = 10$.

The tensile strain in the fibres in the deformed strip are given in Fig. 11. For $C_s = 1$, the maximum tensile strain is equal to 5.39×10^{-4}, i.e. twenty times less than in the case of full integration (Fig. 4). The load necessary to bend the strip is nearly negligible in comparison with full integration (Fig. 12). The computation with $C_s = 1$ is acceptable and the tension locking can be considered to be avoided.

If the parameter C_s is decreased ($C_s = 0.01$, Fig. 11b), the maximum spurious tensile strain decreases to 2.33×10^{-5}. That is very low (and 400 times less than in the case of full integration). The load necessary for the deformation is very close to zero (Fig. 12). If these results are very good, they must be moderated because the top edge of the deformed shape is not completely aligned as it should be.

When the parameter C_s is increased to $C_s = 10$ (Fig. 11c), the maximum fibre strain reaches 1.39×10^{-3} and the load necessary to bend the strip is not negligible (Fig. 12). This parameter is too important and leads to some locking (although much less important than in the case of full integration).

4. Conclusion

The textile composite reinforcements are made up of two fibre directions that enable large in-plane shear deformation by angle variation between warp and weft fibres. This deformation mode is mainly important for draping these materials. The fibres are quasi inextensible and this leads to a tensile locking problem for finite-element analyses when the elements are not aligned with fibre directions. It is not possible to obtain the inextensibility of the fibres at all the Gauss points because of the element kinematics. The phenomenon has been analysed in the present paper, in the case of four node elements on a two-element mesh. Tension locking has also been studied during the deformation of a textile strip on a circular obstacle. This test is well suitable for this analysis because the in-plane shear is continuously variable, from 0° to 60°. An approach has been proposed to avoid tension locking in the case of 4-node quadrilaterals. It combines a one-Gauss-point quadrature and stabilisation on the non-constant part of the in-plane shear strain. This approach can be used in draping simulations to avoid spurious wrinkles in case of non-aligned meshes, in particular when the fibres are not aligned with the edges of the ply.

Several points must be analysed to confirm the efficiency of the approach. In particular, other boundary conditions should be discussed and the optimal value of the C_s coefficient should be verified in a set of tests. This approach does not apply in the case of the three-node triangle for which underintegration is not possible. It is, however, an important point because this triangular element is used in case of automatic meshing and remeshing in the case of complex geometries. This is a main challenge. Other approaches have been used, for instance mixed interpolations in the case of transverse shear locking

of plates and shell elements [21,22]. It will be interesting to analyse if this type of approach can be efficient to avoid tension locking in the case of a triangular element made of textile reinforcements.

Acknowledgement

This research was supported in part by the French Agency for Research (ANR) in the scope of the project MECAFIBRES.

References

[1] P. Boisse (Ed.), Composite Reinforcements for Optimum Performance, Woodhead Publishing Limited, 2011, p. 686.
[2] J.C. Yong, Composites: Application and assessment of market, in: ICCM18 Conference, Jeju, Korea, 2011.
[3] E.R.H. Fuchs, F.R. Field, R. Roth, R.E. Kirchain, Strategic materials selection in the automobile body: Economic opportunities for polymer composite design, Compos. Sci. Technol. 68 (2008) 1989–2002.
[4] C. Douthe, O. Baverel, J.F. Caron, Form-finding of a grid shell in composite materials, J. Int. Assoc. Shell Spat. Struct. 47 (2006) 53–62.
[5] F. Van Der Ween, Algorithms for draping fabrics on doubly curved surfaces, Int. J. Numer. Methods Eng. 31 (1991) 1414–1426.
[6] A.C. Long, C.D. Rudd, A simulation of reinforcement deformation during the production of preform for liquid moulding processes, Proc. Inst. Mech. Eng., B J. Eng. Manuf. 208 (1994) 269–278.
[7] P. De Luca, A.K. Pickett, Numerical and experimental investigation of some press forming parameters of two fibre reinforced thermoplastics: APC2-AS4 and PEI-CETEX, Composites, Part A 29 (1998) 101–110.
[8] S.W. Hsiao, N. Kikuchi, Numerical analysis and optimal design of composite thermoforming process, Comput. Methods Appl. Mech. Eng. 177 (1999) 1–34.
[9] N. Hamila, P. Boisse, F. Sabourin, M. Brunet, A semi-discrete shell finite element for textile composite reinforcement forming simulation, Int. J. Numer. Methods Eng. 79 (2009) 1443–1466.
[10] A.J.M. Spencer, Theory of fabric-reinforced viscous fluid, Composites, Part A 31 (2000) 1311–1321.
[11] X. Peng, J. Cao, A continuum mechanics-based non-orthogonal constitutive model for woven composite fabrics, Composites, Part A 36 (2005) 859–874.
[12] R.H.W. Ten Thije, R. Akkerman, J. Huetink, Large deformation simulation of anisotropic material using an updated Lagrangian finite element method, Comput. Methods Appl. Mech. Eng. 196 (2007) 3141–3150.
[13] P. Badel, S. Gauthier, E. Vidal-Salle, P. Boisse, Rate constitutive equations for computational analyses of textile composite reinforcement mechanical behaviour during forming, Composites, Part A 40 (2009) 997–1007.
[14] X. Yu, L. Ye, Y. Mai, Spurious wrinkles in forming simulations of woven fabric, Int. J. Form. Process. 8 (2005) 141–155.
[15] X. Yu, B. Cartwright, D. McGuckin, L. Ye, Y.W. Mai, Intraply shear locking in finite element analyses of woven fabric forming processes, Composites, Part A 37 (2006) 790–803.
[16] L.R. Hermann, Elasticity equations for incompressible and nearly incompressible materials by a variational theorem, AIAA J. 3 (1965) 1896–1900.
[17] T. Belytschko, W.E. Bachrach, Efficient implementation of quadrilaterals with high coarse-mesh accuracy, Comput. Methods Appl. Mech. Eng. 54 (1986) 279–301.
[18] T. Belytschko, P. Bindeman, Assumed strain stabilization of the 4-node quadrilateral with 1-point quadrature for nonlinear problems, Comput. Methods Appl. Mech. Eng. 88 (1991) 311–340.
[19] T. Belytschko, W.K. Liu, B. Moran, Nonlinear Finite Elements for Continua and Structures, John Wiley & Sons Inc., 2000.
[20] T.J.R. Hughes, T.E. Tezduyar, Finite elements based upon Mindlin plate theory with particular reference to the four-node bilinear isoparametric element, J. Appl. Mech. 48 (1981) 587–597.
[21] E.N. Dvorkin, K.J. Bathe, A continuum mechanics based four-node shell element for general nonlinear analysis, Eng. Comput. 1 (1984) 77–88.
[22] P. Boisse, J.L. Daniel, J.C. Gelin, A C^0 three node shell element for non-linear analysis, Int. J. Numer. Methods Eng. 37 (1994) 2339–2364.
[23] H. Stolarski, T. Belytschko, Membrane locking and reduced integration for curved elements, J. Appl. Mech. 49 (1982) 172–177.
[24] H. Stolarski, T. Belytschko, Shear and membrane locking in curved C^0 elements, Comput. Methods Appl. Mech. Eng. 41 (1983) 279–296.
[25] Q. Zeng, A. Combescure, A new one-point quadrature, general non-linear quadrilateral shell element with physical stabilization, Int. J. Numer. Methods Eng. 42 (1998) 1307–1338.
[26] R.H.W. ten Thije, R. Akkerman, Solutions to intra-ply shear locking in finite element analyses of fibre reinforced materials, Composites, Part A 39 (2008) 1167–1176.
[27] D. Durville, Simulation of the mechanical behaviour of woven fabrics at the scale of fibers, Int. J. Mater. Forming 3 (2010) 1241–1251.
[28] A.K. Pickett, G. Creech, P. de Luca, Simplified and advanced simulation methods for prediction of fabric draping, Eur. J. Comput. Mech. 14 (2005) 677–691.
[29] D.F. Flanagan, T. Belytschko, A uniform strain hexahedron and quadrilateral with orthogonal hourglass control, Comput. Methods Appl. Mech. Eng. 17 (1981) 679–706.
[30] J. Cao, R. Akkerman, P. Boisse, et al., Characterization of mechanical behavior of woven fabrics: Experimental methods and benchmark results, Composites, Part A 39 (2008) 1037–1053.
[31] N. Hamila, P. Boisse, A meso–macro three node finite element for draping of textile composite preforms, Appl. Compos. Mater. 14 (2007) 235–250.